Annales Societatis Geologorum Poloniae (2014), vol. 84: 71–79.

TIME-DOMAIN ELECTROMAGNETIC METHOD IN GEOLOGICAL RESEARCH

Wojciech KLITYŃSKI, Michał STEFANIUK & Juliusz MIECZNIK

AGH University of Science and Technology, Faculty of Geology, Geophysics and Environmental Protection, Al. Mickiewicza 30, 30-059 Kraków, Poland, e-mails: gpklityn@geol.agh.edu.pl; stefan@geol.agh.edu.pl; j_miecznik@poczta.onet.pl

Klityński, W., Stefaniuk, M. & Miecznik, J., 2014. Time-domain electromagnetic method in geological research. *Annales Societatis Geologorum Poloniae*, 84: 71–79.

Abstract: This paper describes the theoretical basis of the time-domain electromagnetic method (TDEM) and its application in geological research. The paper discusses the behavior of the electromagnetic field of pulse current sources (magnetic dipole) in the near zone. The problem of the penetration depth of the TDEM method is discussed, in the context of its application in geological research and to gas exploration in the Rudka Gas Field, located in the Carpathian Foredeep. The TDEM sounding curves from the Rudka Field and the influence of noise on the penetration depth are discussed. A 1-D Occam inversion of TDEM soundings was obtained for a profile across the borehole A-10. An integrated (TDEM and borehole) interpretation of the data was made and a 2-D resistivity cross-section was obtained along the profile, as a contribution to geological reconnaissance for gas prospecting.

Key words: Time-domain electromagnetic method, near zone, apparent resistivity, penetration depth, hydrocarbon prospecting.

Manuscript received 6 November 2013, accepted 3 March 2014

INTRODUCTION

The time domain electromagnetic method (TDEM), employs the electromagnetic field that is generated by rectangular current pulses (see Appendix, Fig. 6), modified by the transient processes taking place in a conducting medium, such as rock, which can be described by means of the Heaviside step function (see Appendix, formula 7). With its facilitation technologies, the TDEM is very useful in geological investigations. EM field properties usually are discussed for two areas: the near zone (induction) and the far zone (radiation).

The near zone refers to the region, in which the distance, r, between transmitter loop (T) and receiver coil (R) is many times less than the wave length λ ($r << \lambda$) (see Appendix, formula 1); in practical terms this holds true for small values of r and a low-frequency EM field (Kaufman and Keller, 1981). The transmitter loop in TDEM is usually a square wire loop with a side L, while the receiver coil has a diameter a (see Appendix, Fig. 7). Bearing in mind the fact that the wave length ranges from a few to several tens of thousands of metres (see Appendix), the TDEM measurements are carried out in the near zone. The condition $r >> \lambda$ must be satisfied in the far zone. In the near zone, the biggest contribution to EM field intensity at a distance r from the transmitter change according to $1/r^2$ and $1/r^3$, i.e., the EM field decreases abruptly with an increase in distance. In the far zone, the EM field intensity decays slowly, because the biggest contribution to it is from 1/r (Kaufman and Keller, 1981).

A particular case of measurement in the near zone is when the receiving coil is located centrally inside the transmitting loop, i.e., r = 0 (central loop) (see Appendix; Fig. 8). In this case, the effects of 2-D and 3-D lateral objects on the magnetic field are smaller and as a result the accuracy of interpretation around the measurement dipole is greater. As in other geoelectric methods, the results are presented as sounding curves, i.e. plots of apparent resistivity ρ_a versus time, t, where t is measured, starting from the turn-off of the current pulse, and as plots of voltage measured in the receiving coil, as a function of that time (see Appendix, formula 24; Fig. 10).

Since it has a high resolution, in some applications the transient electromagnetic method is often more effective than the resistivity method, e.g. in mapping contaminated water zones (Antoniuk *et al.*, 1991). The TDEM also has a higher resolution that other electromagnetic methods (Barrocu and Ranieni, 2000). The prospecting capability of TDEM is presented in a case study of the Rudka gas accumulation, where the TDEM was applied in hydrocarbon exploration.

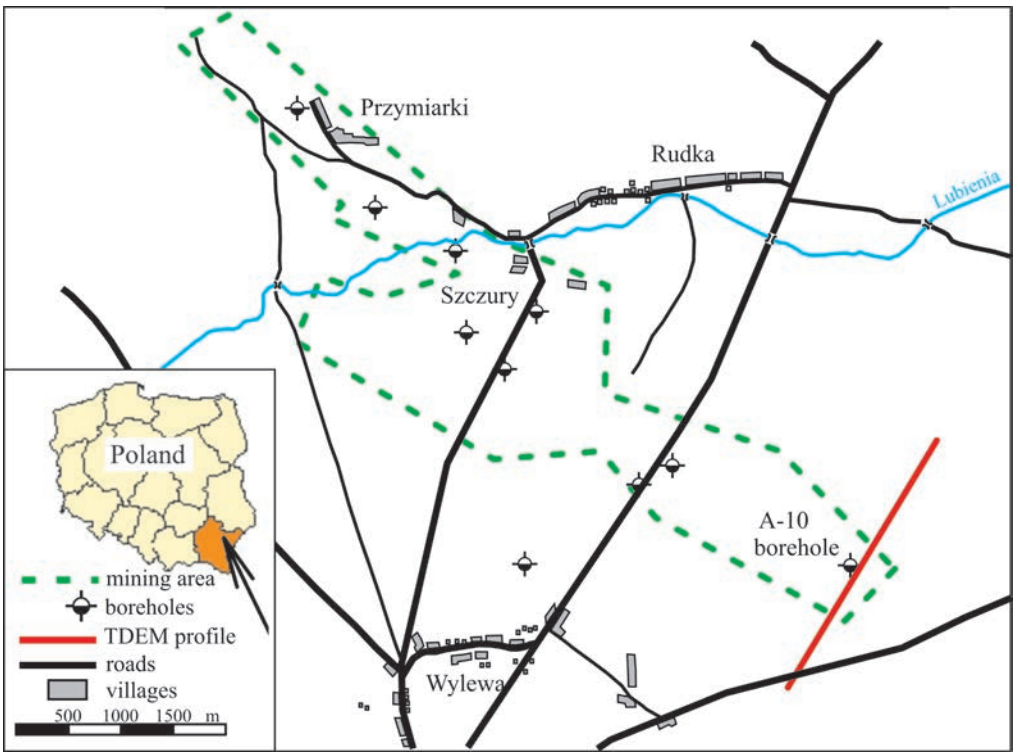

Fig. 1. Location of TDEM profile 02-R-09.

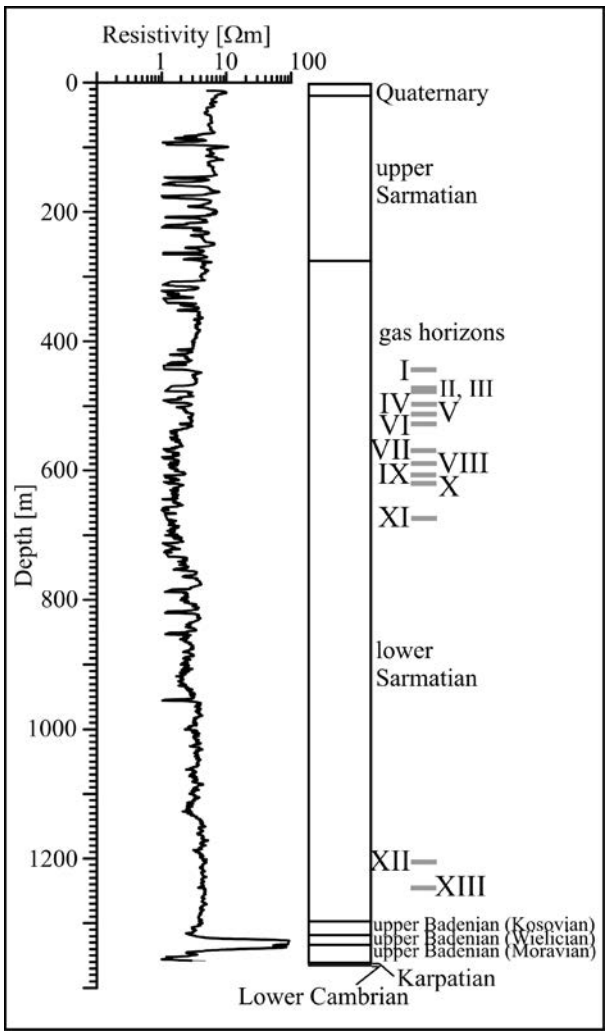

The capability for using different components of the electric field and magnetic field, as well as different EM field sources (electric dipole, magnetic dipole) and receivers, allows measurement techniques to be adjusted in individual prospecting problems. A variety of available measurement techniques contributes to the greater efficiency of EM methods, when applied to solving structural and reservoir problems.

To obtain a TDEM depth penetration of about 1,000 m, it is enough to use a square transmitting loop with a side of 500 m, with a receiving coil placed inside the loop (see Appendix, Fig. 8), while in the CSAMT (see Appendix) that uses an EM field in the far zone (i.e., $\lambda << r$), the transmitter-receiver distance must be at least three times the required and possible penetration depth and the limited penetration depth for a low-resistivity medium (see Appendix) (Zonge, 1992a).

The TDEM option, in which the receiving coil is located inside the transmitting loop (the near zone), is used for a number of prospecting problems in engineering geology, the geology of mineral deposits, hydrogeology, and studies of tectonics (Klityński and Targosz, 2011a, b). The TDEM option, measuring changes in the vertical component of the magnetic field with time, can be applied over a wide depth range: from a few to a thousand or more metres (Keller, 1997).

Fig. 2. Resistivity plots obtained from electric logs and simplified geological profile for borehole A-10 (location: Figure 1).

EXAMPLE OF TDEM MEASUREMENTS AND THEIR APPLICATION IN GAS FIELD OF CARPATHIAN FOREDEEP

TDEM measurements at the Rudka gas accumulation in the Carpathian Foredeep were made by the Geophysical Exploration Company, Warsaw. The goal was to examine the applicability of the TDEM to hydrocarbon prospecting. The gas accumuklation is located in the NE part of the Carpathian Foredeep. It is a multi-horizon gas field in sandstone-shale layers of Lower Sarmatian age. The effective thickness of gas-bearing layers ranges from a few to several dozen meters. Figuła *et al.* (2010) described the discovery and development of the field.

Gas horizons occur in a depth range of 450 to 1,200 m. Since the sandstones contain a lot of clay, resistivity contrasts between the reservoir and sealing rocks are poor (Wojdyła *et al.*, 2011). Resistivity logs for well A-10 (for location see Fig. 1) show small resistivity contrasts within the gas-bearing intervals (Fig. 2). The gas-saturated sandstones are difficult to identify by EM methods, because they occur as thin layers. The thin layers of shale and sandstones are only weakly identifiable by means of surface geophysical methods (Stefaniuk, 2011). The higher resistivity of the sandstones, as compared to the surrounding rocks, is employed in hydrocarbon prospecting (Klityński and Targosz, 2011b).

TDEM measurements, version MulTEM (see Appendix), were made at the Rudka Gas Field, using the Phoenix Geophysics system V8, with a transmitting loop size of L = 200 m, 500 m, current intensity 30 A, and frequency of pulse source of 1 Hz. TDEM sounding curves were obtained for a time range of 2.68 to 213 ms (see Appendix, Fig. 10; Stefaniuk *et al.*, 2011). The receiver output voltage unit is [nV/Am2] (see Appendix, Fig. 10A).

This paper is a continuation of previous work focused on application of the TDEM method for oil and gas exploration (Klityński and Targosz, 2011a).

Measurements were carried along a profile of 2,300 m length (Fig. 1). First, six TDEM soundings (No R9_91–R9_87) were made with a transmitter loop side of L = 200 m. Then, owing to strong noise, the TDEM measurement was modified and 86 soundings were made, with the use of a big transmitting loop with the side L = 500 m (soundings R9_86–R9_92).

Strong effects of noise on receiver voltage is observed for a transmitter loop L = 200 m. For a time interval of 134 to 213 ms, the voltage value is smaller than the noise (see Appendix and Fig. 3A). Constricting the use of sounding curves to a time of 106 ms (Fig 3) markedly limits the penetration

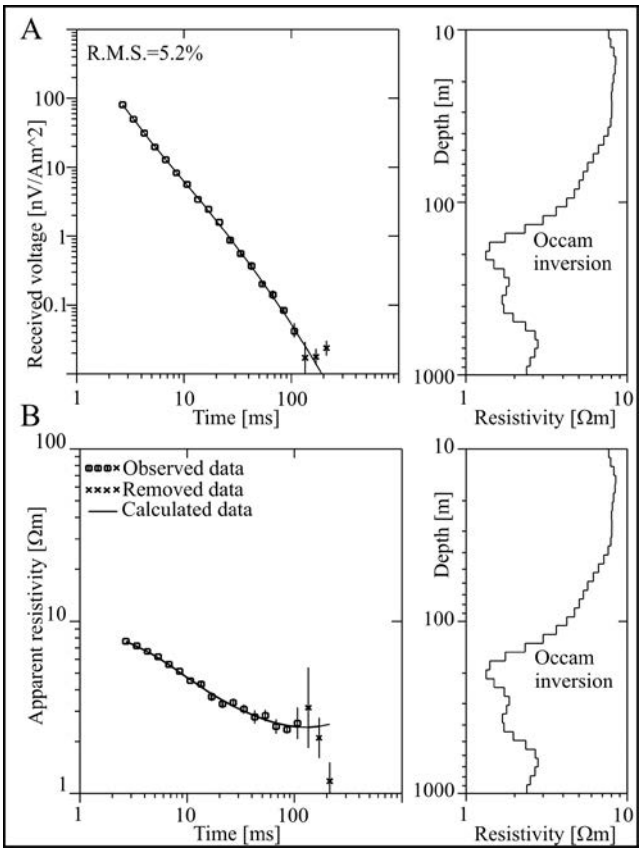

Fig. 3. Result of simultaneous Occam inversion of apparent resistivity curves and receiver output voltage (B) of TDEM sounding No R9_91 from profile 02-R-09 (transmitter loop L = 200 m, time range 2.68–213 ms).

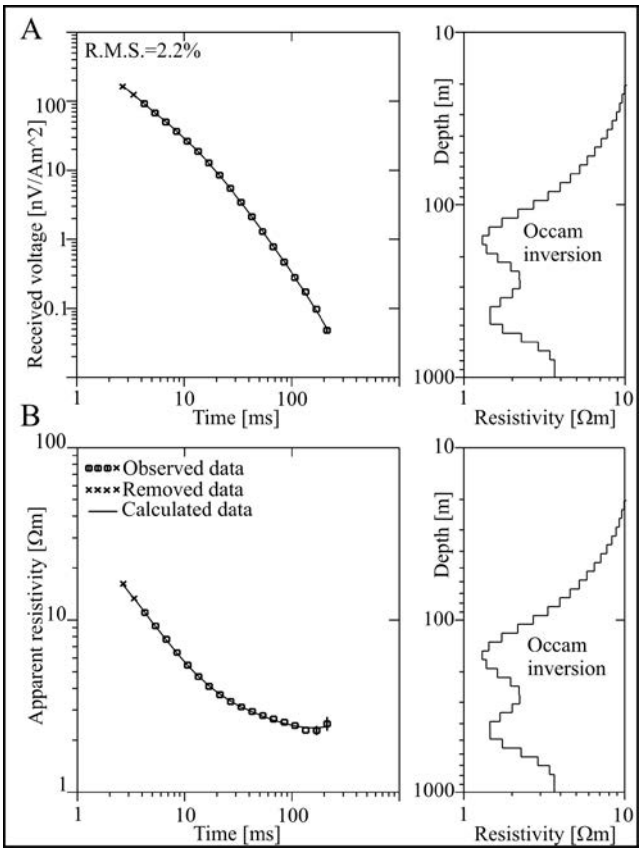

Fig. 4. Result of simultaneous Occam inversion of apparent resistivity curves and receiver output voltage (B) of TDEM sounding No R9_49 from profile 02-R-09 (transmitter loop L = 500 m, time range 2.68–213 ms).

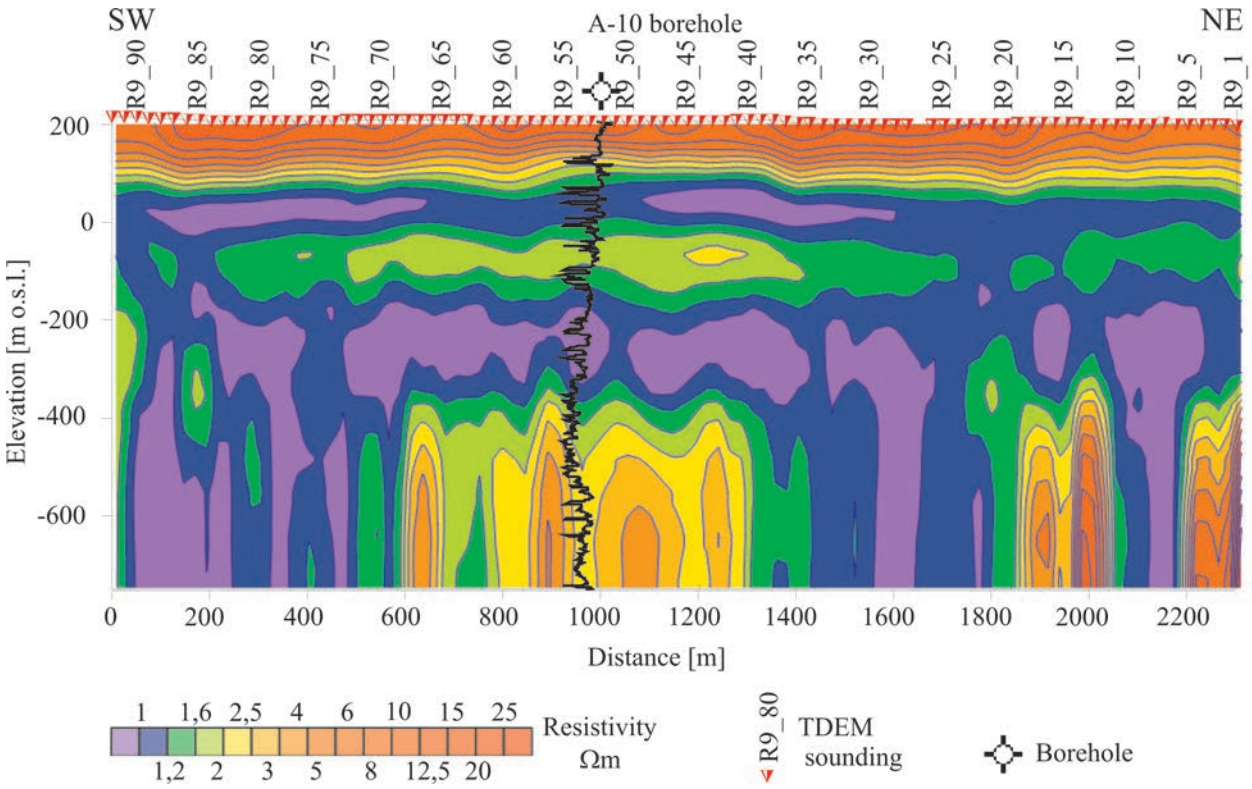

Fig. 5. Pseudo-2-D resistivity cross-section as a result of Occam inversion along profile 02-R-09.

depth and the prospecting capabilities of the method. Measurements were made on the profile 02-R-09 with a measurement step of 25 m and hence the length of profile section was 125 m there (SW part of the profile, Fig. 1). This part of the profile is outside of the documented reservoir horizon. Assuming that the average resistivity of the medium is 3 m (based on resistivity logs from well A-10; Fig. 2), the penetration depth is about 700 m (see Appendix, formula 6).

The noise level can be evaluated from the receiver output voltage, changing with time (Fig. 3A) at about $\eta_v = 0.1$ nV/m^2 (regarding that transmitter current is 30 A). According to formula 21 (see the Appendix), the penetration depth is also about 700 m and this is evidence of the effect of noise. To effectively map gas horizons I–IX (Fig. 2), the penetration depth should be equal to about 1,000 m and therefore the receiver voltage U(t) should be higher than noise. To achieve this, the magnetic moment M_t of the transmitter loop must be increased (see Appendix, formula 21).

Therefore, subsequent measurements were carried out using a transmitter loop with the greater side, L = 500 m and the sounding curves were almost undisturbed (Fig. 4). According to formula (21) (see Appendix), the penetration depth at noise $\eta_v = 0.1$ nV/m^2 is about 1,100 m. As can be seen, the maximum recording time of 213 ms and small noise effects (Fig. 4) guarantee that the penetration depth exceeds 1,000 m. This results in more effective reservoir interpretation than in the case of a small transmitter loop.

The quantitative interpretation of TDEM sounding curves from profile 02-R-09 was performed by means of the Occam inversion. The MulTEM version of TDEM uses the fact that effects of 2-D and 3-D side objects are small and therefore a 1-D medium can be assumed in the interpretation, i.e., resistivity varies only vertically (see Appendix).

However, the Occam inversion is the most objective. Because of its specificity, one cannot obtain sharp geoelectric boundaries; the boundaries are unclear (Constable *et al.*, 1987). The results of the Occam inversion can be presented separately for each sounding curve as graphs of resistivity distribution with depth (Figs 3, 4). However, the best form of presentation for the 1-D Occam inversion results is as pseudo-2-D cross-sections of the resistivity distribution along the profile (Fig. 5). The identification of geological boundaries is based on resistivity logs and geological data.

The uppermost part of geological section, i.e. to 200–250 m below the ground surface (about 50 m below sea level), is built of flat layers with a relatively uniform resistivity (Fig. 5). Two layers can be distinguished there: the upper layer, with higher resistivity (several dozen m), and the lower, low-resistivity one (a few m). The layers are composed of Quaternary and Upper Sarmatian rocks. At higher levels, sandstones occur, while below there are shales. Deeper, at a depth interval of –50 to –150 m below sea level, there is another layer with intrinsic diversity and higher resistivity, which can be related to the youngest deposits of the Lower Sarmatian. The resistivity distribution suggests that the lithology and facies development of the deposits are varied. Pockets of rocks with increased resistivity are probably related to the sediments of buried river beds.

Beneath there is a low-resistivity shale complex with a thickness of about 100 m that acts as the main sealing horizon. Deeper down, the gas horizon extends to about 800 m

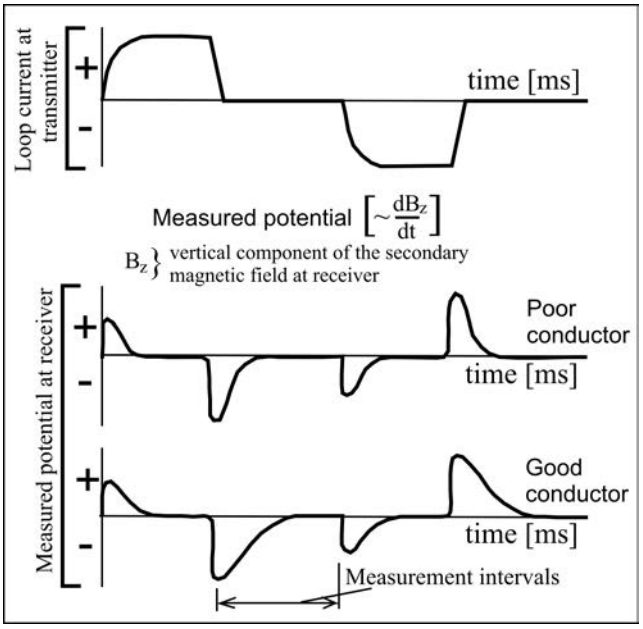

Fig. 6. Generalized scheme of TDEM system: time series/ waveforms for transmitter current and measured potential.

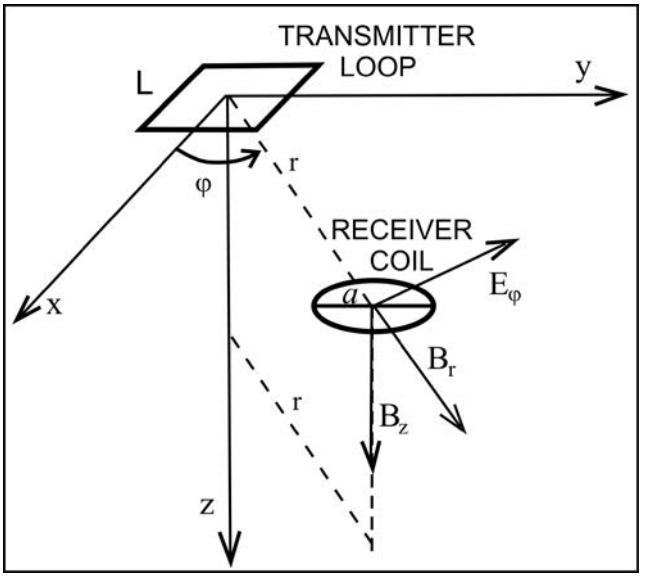

Fig. 7. EM field components of magnetic dipole in cylindrical co-ordinate system.

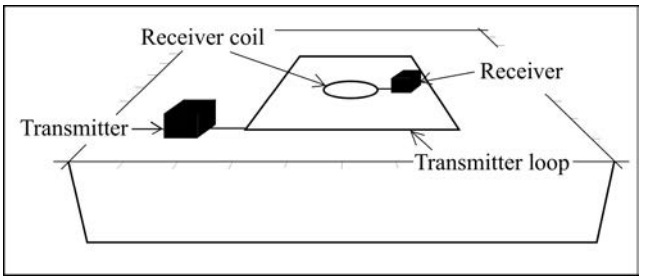

Fig. 8. Measurement system configuration for TDEM; central-loop configuration (Zonge, 1992b).

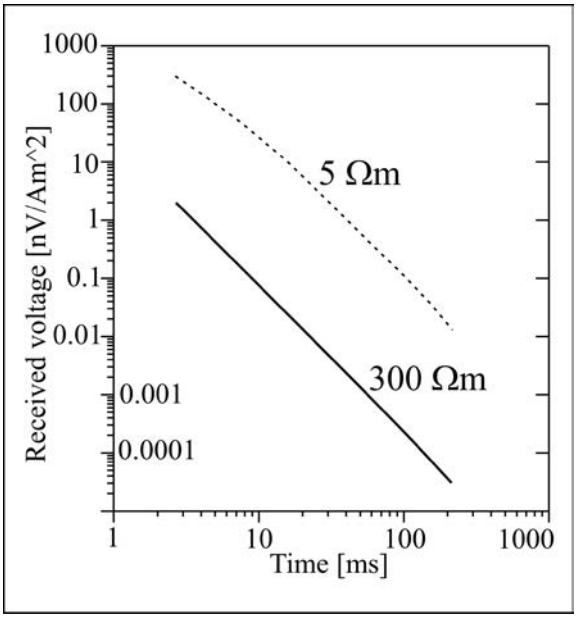

Fig. 9. Receiver output voltage calculated for homogeneous medium with resistivity: 5 m and 300 m.

below sea level. The gas-saturated sandstones are difficult to identify there, because they occur as thin layers that are poorly discernible using surface methods. Gas horizons I–V (Fig. 2) at a depth interval of 450 to 500 m have the small thickness of 2–4 m. Owing to the limited resolution of TDEM, those horizons are not visible in the resistivity cross-section (Fig. 5). The lower horizons, VI–XIII (Fig. 2), have a greater thickness, from a few to several dozen meters. They can be observed in the cross-section as an internally diverse, broad zone with higher resistivity, which takes the form of an anticline, 1,000 m in width, at a depth of 550 m below the surface (Fig. 5).

The results of the quantitative Occam inversion, presented as the resistivity distribution with depth (Figs 3, 4) and pseudo-2-D resistivity cross-sections (Fig. 5), show that TDEM has good prospecting capabilities. Despite the small resistivity contrasts, it is possible to identify the reservoir zone, which has gas horizons (eight) interbedded with sealing layers at a depth range of 550 to over a thousand metres, and a thickness of a dozen to a few dozen metres. Gas-bearing horizons with higher resistivity (several dozen m), together with low-resistivity sealing layers (a few m), form a composite layer with a higher resistivity of several m (Fig. 5). Therefore, the TDEM method can be applicable to hydrocarbon prospecting to a depth of 1,000 m, even if there are small resistivity contrasts in the study area.

CONCLUSIONS

The most important outcomes of our study are summarised below:

1. The TDEM method is efficient in investigations of geological sections with low resistivity. High resistivity causes the signal measured to be weaker than the sensitivity of the measurement equipment and/or the noise level.

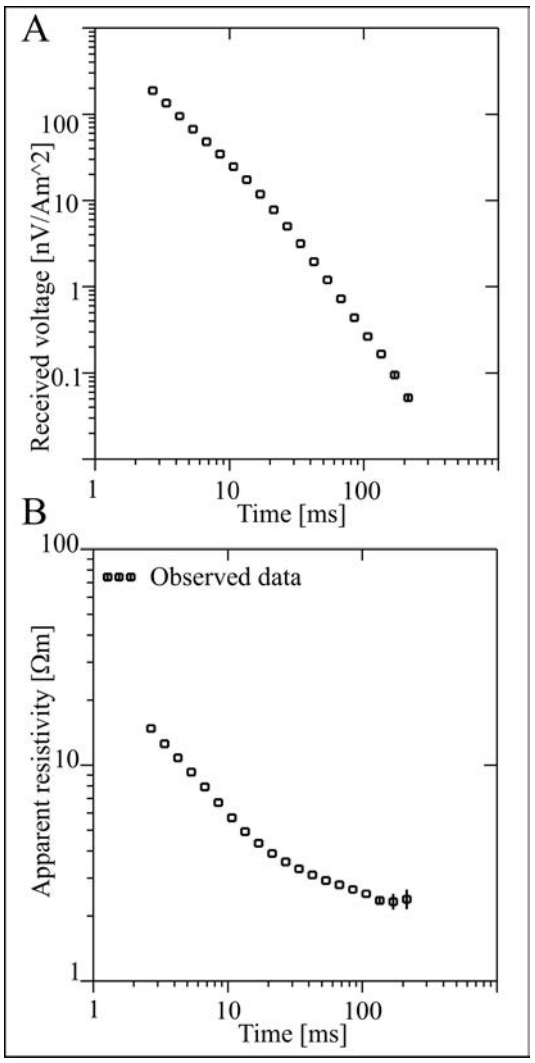

Fig. 10. Examples of TDEM sounding curves from profile 02-R-09. **A.** Receiver output voltage as a function of time. **B.** Apparent resistivity as a function of time.

2. Time derivative of the vertical component of the magnetic induction vector in the near zone does not depend on the transmitter-receiver distance, T-R. Therefore, one can interpret geo-electric cross-sections at depths greater than the distance T-R. Neither electromagnetic methods that use harmonic fields nor resistivity method are capable of this.

3. The ability to interpret TDEM measurements in the near zone can significantly reduce the costs and time of measurement, compared to other geo-electric investigations. Owing to the minor influence of 2-D and 3-D lateral geological objects on the measured EM field, the TDEM interpretation in the near zone is more effective and one-dimensional interpretation procedures can be applied with great accuracy.

4. The TDEM penetration depth depends on the maximum measurement time, at which the signal can be recorded. Measurement time can be prolonged by increasing the transmitter loop size and the source power. The maximum measurement time is restricted by the noise level on one side and by resistivity on the other side. The EM wave decays faster at low resistivities, while the receiver output voltage drops rapidly at high resistivities (see Appendix, Fig. 9). Therefore, the resistivity of a medium restricts the TDEM capabilities.

5. The TDEM penetration depth is strongly limited by noise. It is therefore necessary to employ large-size, high-power transmitting loops, in order to enhance the magnetic moment of the receiver. This amplifies the receiver output voltage and as a result reduces the effects of noise on measurement.

6. The MulTEM version of TDEM employing a big transmitting loop (e.g., 500×500 m^2) and a strong current source (e.g., 30 A) can be applied to hydrocarbon prospecting in the Carpathian Foredeep.

Acknowledgements

The paper was prepared as contribution to research no: 11.11.140.322 in the Department of Fossil Fuels, Faculty of Geology, Geophysics and Environmental Protection. It presents some of the results of the project: "Elaboration of innovative methods of discovery of hydrocarbon deposits and recognition of the structure and variability of deposits during its exploitation with use of complex of deep and medium range electromagnetic surveys", financed by the Ministry of Science and Higher Education in the framework of Scientific Research Project No. 1302. The authors express their gratitude to the reviewers, Vladimir Semenov and Jerzy Sobotka, for their valuable and prompt feedback. Their comments significantly improved the quality of the paper.

REFERENCES

Antoniuk, J., Maćkowski, T. & Klityński, W., 1991. Analiza rozdzielczości krzywych sondowań elektrooporowych i procesów przejściowych w aspekcie monitorowania zanieczyszczeń wód podziemnych. In: Stefaniuk M. (ed.), *Materiały III Krajowej Konferencji Naukowo-Technicznej pt. "Zastosowanie metod geofizycznych w górnictwie kopalin stałych"*, Jaworze, 28-30 listopada 1991. Wydawnictwo Akademii Górniczo-Hutniczej, Kraków, t. 2, p. 109–126. [In Polish.]

Barrocu, G. & Ranieri, G., 2000. TDEM: A useful tool for identifying and monitoring the fresh-saltwater interface. In: Sadurski, A. (ed.), *Hydrogeology of the Coastal Aquifers*. Proceedings of the 16th Salt Water Intrusion Meeting, Międzyzdroje-Wolin Island (Poland), 12–15 June 2000. Nicolaus Copernicus University, Toruń, p. 9–15.

Bracewell, R. N., 1965, *The Fourier Transform and Its Applications*. McGraw-Hill Book Co., New York, 203 pp.

Constable, S. C., Parker, R. L. & Constable, C. G., 1987. Occam's inversion: A practical algorithm for generating smooth models from electromagnetic sounding data. *Geophysics*, 52: 289–300.

Figuła, J., Stefaniuk, M., Wojdyła, M. & Sito, Ł., 2010. Przestrzenny model elektromagnetyczny południowo-wschodniej części złoża Rudka. In: Stefaniuk, M. (ed.), *Opracowanie nowatorskich metod wykrywania złóż węglowodorów oraz rozpoznawania struktury i zmienności złóż w trakcie ich eksploatacji za pomocą kompleksu głębokich i średniozasięgowych badań elektromagnetycznych*, Materiały Seminaryjne, Iwkowa, 23–25 listopada 2010, Ministerstwo Nauki i Szkolnictwa Wyższego, p. 22–23. [In Polish.]

Gasanienko, L. B., 1958. Normalnoe pole vertikalnogo harmoni-

cheskogo niskochastnogo magnitnogo dipola. *Vaprosy Geofizyki*, 249: 15–36. [In Russian.]

Kaufman, A. A. & Keller, G. V., 1981. *The Magnetotelluric Sounding Method*. Elsevier, Amsterdam, 595 pp.

Kaufman, A. A. & Keller, G. V., 1983. *Frequency and Transient Soundings*. Elsevier, Amsterdam, Methods in Geochemistry and Geophysics, 685 pp.

Keller, G.V., 1997. Principles of time-domain electromagnetic (TDEM) sounding. *The Leading Edge*, 16: 355–357.

Klityński, W. & Targosz, P., 2011a. Principles of the transient electromagnetic method and possibilities of its application to oil and gas exploration. *Geologia*, 37: 89–111. [In Polish, English summary.]

Klityński, W. & Targosz, P., 2011b. Applying of the transient electromagnetic method to exploration of oil and gas fields In the area of Grabownica Starzeńska-Humniska-Brzozów. *Geologia*, 37: 141–156. [In Polish, English summary.]

Lebiediev, N. N., 1957. *Funkcje specjalne i ich zastosowanie*. PWN, Warszawa, 303 pp. [In Polish.]

Phoenix Geophysics, 2006. *System 2000.net User Guide, Version 3.0.* Phoenix Geophysics Limited, 3781 Victoria Park Avenue, Toronto, Canada, 324 pp.

Simpson, F. & Bahr, K., 2005. *Practical Magnetotellurics*. Cambridge University Press, Cambrigde,United Kingdom, 270 pp.

Spies, B. R., 1989. Depth of investigation in electromagnetic sounding methods. *Geophysics*, 54: 872–888.

Stefaniuk, M., 2011. Electromagnetic methods in petroleum prospecting. *Geologia*, 37: 5–36. [In Polish, English summary.]

Stefaniuk, M., Bartuś, T., Figuła, J., Górecki, W., Ilewicz-Stefaniuk, D., Klityński, W., Maćkowski, T., Maj, E., Mastej, W., Miecznik, J., Papiernik, B., Putynkowski, G., Rajcher, B., Sada, M., Sito, Ł., Słonka, T., Targosz, P. & Wojdyła, M., 2011. Opracowanie nowatorskich metod wykrywania złóż węglowodorów oraz rozpoznawania struktury i zmienności złóż w trakcie ich eksploatacji za pomocą kompleksu głębokich i średniozasięgowych badań elektromagnetycznych. In: Stefaniuk, M. (ed.), *Sprawozdanie wyników badań wykonanych w ramach projektu naukowo-badawczego nr 1302 finansowanego przez Ministerstwo Nauki i Szkolnictwa Wyższego,* Akademia Górniczo-Hutnicza, Kraków, 520 pp. [Unpublished report, in Polish.]

Wojdyła, M., Stefaniuk, M., Sada, M. & Sito, Ł., 2011. Induced polarization method in hydrocarbon prospecting. *Geologia*, 37: 63–88. [In Polish, English summary.]

Zonge, K. L., 1992a. Introduction to CSAMT. In: Van Blaricom, R. (ed.), *Practical Geophysics II*, for the Exploration Geologist. Northwest Mining Association, Spokane, Washington, USA, 7 pp.

Zonge, K. L., 1992b. Introduction to TDEM. In: Zonge, K. L. (ed.), *Practical Geophysics II*, Northwest Mining Association. Zonge Engineering and Research Organization Inc, Tucson, Arizona, USA, 7 pp.

APPENDIX

The EM wave length in a rock medium is expressed (Kaufman and Keller, 1981) as:

$$\frac{2}{|k|} \tag{1}$$

where k is so-called wave number, which is a complex number in the form (Kaufman and Keller, 1981):

$$k^2 \quad ^2 \quad i \tag{2}$$

where 2 w is angular frequency [1/s], f is EM frequency [Hz],
is permittivity [F/m], is permeability [H/m],
is conductivity of a medium [S/m], where 1/ and is resistivity [m].

For a low EM field frequency (here: 1 Hz) and assuming that H/m, where $_o$ 4 10^{-7} is permeability of free space, the wave number can be expressed in the form (Simpson and Bahr, 2005):

$$k^2 \quad i \quad _o \tag{3}$$

Hence, for a conductivity σ, ranging from 1 to 0.01 S/m, and a frequency of 1 Hz, the wave length (λ) ranges from about 2,000 to about 20,000 m.

EM methods use the electric field and the magnetic field that are produced by a current, which is varying with time. The current variation with time can be expressed by a harmonic form $e^{\ i\ t}$ or by the Heaviside unit function, describing a pulse current. The first case refers to Frequency Domain Electromagnetics (FDEM) e.g., Control Source Audio-frequency Magnetotellurics (CSAMT) (Zonge, 1992a); the other one refers to transient electromagnetics, TDEM (Zonge, 1992b).

Electromagnetic penetration depth depends mostly on the damping of electric and magnetic amplitude in a conductor. In the frequency domain, the EM penetration depth (δ_{FD}) in a conducting medium can be evaluated from the so-called skin effect depth, i.e., the depth at which the EM field decays to 1/e or 37 % of its surface value. Then the formula has the form (Spies, 1989):

$$_{FD} \quad \sqrt{\frac{2}{_o}}\,[\mathrm{m}] \tag{4}$$

This formula is often written in a simplified form:

$$_{FD} \quad 500\sqrt{\frac{}{\mathrm{f}}} \quad \frac{500}{\sqrt{\quad \mathrm{f}}} \tag{5}$$

It can be seen that the penetration depth decreases with increasing conductivity (σ) and frequency (f). For a resistivity of 3 m (here) and a frequency of 1 Hz (in CSAMT practically little bigger), the penetration depth is about 850 m.

The EM field penetration depth in the time domain (δ_{TD}) is calculated from (Spies, 1989):

$$_{TD} \quad \sqrt{\frac{2t_{\max}}{_o}} \tag{6}$$

where t_{max} is the maximum measurement time, at which a voltage can be measured, i.e. when the voltage is greater than noise at a measurement site (Spies, 1989). The recording time t is measured from the cut-off of the current pulse in the transmitter (Fig. 6). According to the diffusion rule, the longer the maximum measurement time (t_{max}), the bigger the penetration depth.

The TDEM method uses the stabilization of Earth's electromagnetic field induced by transient pulses of electric current, which are transmitted to an ungrounded loop (Fig. 6).

The EM field is recorded in the time domain (Kaufman and Keller, 1983). Let the primary field be generated by a vertical magnetic dipole induced with the current intensity, described by the Heaviside step function (Bracewell, 1968):

$$F(t) \quad \begin{matrix} 0 \text{ dla } t \quad 0 \\ 1/2 \text{ dla } t = 0 \\ 1 \text{ dla } t \quad 0 \end{matrix} \tag{7}$$

where t is time.

Such a dipole can be obtained by laying out on the ground a square loop with side L made from a single coil or multi- coil.

The electromagnetic field, produced by such a dipole, has the following components (Fig. 7) on the surface of the uniform half-space (Gasanienko, 1958):

$$E \quad \frac{3M_t}{2 \quad r^4} e \qquad [\text{V/m}] \tag{8}$$

$$B_z \quad \frac{{}_o M_t}{4 \quad r^3} b_z \quad [\text{T}] \tag{9}$$

$$B_r \quad \frac{{}_o M_t}{4 \quad r^3} b_r \quad [\text{T}] \tag{10}$$

where:
E – azimuthal component of electric field
B_z – vertical component of magnetic induction field
B_r – radial component of magnetic induction field
r – distance between transmitter loop (T) and receiver coil (R)
Mt = I·S·n – magnetic moment of transmitter loop
I – intensity of pulse current
S – surface of transmitter loop
n – number of coils in transmitter loop
V– Volt and T – Tesla

$$e \qquad u \quad \sqrt{\frac{2}{}} u \quad 1 \quad \frac{u^2}{3} \quad e^{\,u^2/2} \tag{11}$$

$$b_z \quad 1 \quad 1 \quad 9u^{\,2} \quad u \quad \sqrt{\frac{2}{}} \quad \frac{9}{u} \quad 2u \quad e^{\frac{u^2}{2}} \tag{12}$$

$$b_r \quad 4e^{\frac{u^2}{4}} \quad 2 \quad \frac{u^2}{4} \; I_1 \; \frac{u^2}{4} \quad \frac{u^2}{4} I_o \; \frac{u^2}{4} \tag{13}$$

where:

$$u \quad \sqrt{\frac{2}{}} \int_0^u e^{\frac{t^2}{2}} dt \tag{14}$$

is a probability integral:

$$u \quad \frac{2 \quad r}{}; \qquad \sqrt{\frac{8^{\,2} \quad t}{o}} \quad \sqrt{2 \quad 10^7 \quad t} \tag{15}$$

As is the wave length and r is the distance T-R, so u defines whether the measurement is in the near zone or the far zone; I_o and I_1 are the modified Bessel functions (Lebiediev, 1957).

Let us calculate time derivatives of vertical and radial components of the magnetic induction vector. Taking into account relations (10) and (11), we get:

$$\frac{}{t} B_z \quad \frac{M_t}{4 \quad r^3} \frac{}{t} b_z \tag{16}$$

$$\frac{}{t} B_r \quad \frac{M_t}{4 \quad r^3} \frac{}{t} b_r \tag{17}$$

As u and $\phi(u)$ depend on time, derivatives $\frac{}{t} b_z$ and $\frac{}{t} b_r$ are calculated from formulas:

$$\frac{}{t} b_z \quad \frac{b_z}{u} \frac{}{t} u \; ; \quad \frac{}{t} b_r \quad \frac{b_r}{u} \frac{}{t} u \; ; \qquad \frac{}{t} \quad u \quad \sqrt{\frac{2}{}} e^{\frac{u^2}{2}} \tag{18}$$

Relations (11) through (17) show that the decay of an EM field generated by a pulse current depends on the ratio r/ . Let us study the character of the field for small values of r/ , i.e., when $u \to 0$, with regard to measurement techniques. This is the region of a small distance T-R and late-time EM pulse propagation.

The region, in which $u \to 0$, is called the near zone. Bearing in mind relationships (16) and (17) and taking the conditions in the near zone, after the appropriate transformations, we get the time derivative of the vertical component of the magnetic induction vector:

$$\frac{}{t} B_z \quad \frac{M_t}{20 \sqrt{\quad}} \frac{}{t^{5/2}} \tag{19}$$

This formula shows that time variations of the vertical component of the magnetic induction vector in the near zone do not depend on the T-R distance. This characteristic feature of the magnetic field of a pulse source is of great practical importance. It allows measurements to be made for T-R distances that are much smaller than in other EM methods, in which time-dependent harmonic sources are used.

A special case of the near zone, discussed in this paper, is when the receiver coil is placed in the geometrical centre of the transmitting loop, i.e., r = 0. The measurements then are less affected by lateral objects and as a result, the accuracy of interpretation of the geoelectric cross-section near the measurement array is higher. So, at the late-time EM pulse (big value of) the EM field propagates uniformly in the space between the field source and the registration site. The EM field amplitude decays evenly with time. Therefore, it is possible to investigate deep-seated objects in close proximity to the pulse source.

The central loop array is shown on figure 8 (Zonge, 1992b). A version of such an array is MulTEM, in which the receiver coils are located within the transmitting loop along

the profile. The Geophysical Exploration Company, Warsaw, uses the Phoenix V8 system for their measurements (Phoenix Geophysics, 2006).

When the source of EM field is a transmitting loop, the TDEM measures voltage (U)t in the receiving coil:

$$U\,t \quad \frac{B_z}{t} \tag{20}$$

Formula 19 shows that the TDEM is more sensitive to conductivity changes than other EM methods are (the voltage is proportional to $^{3/2}$). It also can be observed that the receiver output voltage decreases with time, so that it can be smaller than instrument's sensitivity. Therefore, to increase the measured voltage one should increase the transmitter magnetic moment (M_t). The penetration depth of the TDEM is limited by the medium's low conductivity, owing to enhanced attenuation of the EM field (6) and the length measurement time, as the voltage is inversely proportional to time (19). Hence, TDEM penetration depth is a more complex problem than the diffusion rule says. It depends on source power, transmitter loop size, the medium's resistivity and the noise at a measurement site (Spies, 1989).

The penetration depth of a system in the near zone can be evaluated from the formula (Spies, 1989):

$$D_{TD} \quad 0.55 \quad \frac{M_t}{}^{1/5} \tag{21}$$

where is noise at the measurement site, usually ranging from 0.1 to 10 nV/m2 (Spies, 1989). The maximum recording time (at which it is possible to measure a signal) is (Phoenix Geophysics, 2006):

$$t_{max} \quad {}_0 \quad \frac{Mt/Nm^{\,2}}{400^{\,3}}^{1/5} \quad s \tag{22}$$

The penetration depth is also affected by the resistivity. The output voltage drops faster in a poorly conducting medium (equations: 19, 20). Assuming that noise is Nm = 0.1 nV/m2 for magnetic moment Mt = 30·500·500 Am^2, the maximum time at average resistivity of 5 m is ca 400 ms while at 300 m the time is as low as 35 ms (formula 22) (Fig. 9).

The results of theoretical calculations and measurement data for TDEM are presented as sounding curves, i.e. plots of receiver output voltage (U(t)) and apparent resistivity ($_a$(t)) as a function of turn-off time (Figs 10A, 10B).

Using formula (19), the apparent resistivity can be described as (Kaufman and Keller, 1983):

$$\frac{a}{1} \quad \frac{\dot{B}_z^{\,o}}{\dot{B}_z} \tag{23}$$

where $\dot{B}_z^{\,o}$ – time variations of the vertical component of magnetic induction vector in the homogeneous half-space; $\dot{B}_z$ – time variations of the magnetic induction vector in the rock medium; $_1$ – resistivity of the first subsurface layer.

The apparent resistivity sounding curves are calculated from (Kauffman and Keller, 1983; Phoenix Geophysics, 2006):

$$a \quad \frac{0}{4} \quad \frac{2 \quad {}_0 M_t}{5\,U\,t\,/S_r}^{2/3} \quad t^{\,5/3} \tag{24}$$

where S_r – effective surface of receiver coil [m^2].